

Word Confidence Using Duration Models

Original

Word Confidence Using Duration Models / Scanzio, S; Laface, Pietro; Colibro, D; Gemello, R.. - (2009), pp. 1207-1210. (Interspeech 2009 Brighton 6-10/9/2009).

Availability:

This version is available at: 11583/2280631 since:

Publisher:

ISCA

Published

DOI:

Terms of use:

This article is made available under terms and conditions as specified in the corresponding bibliographic description in the repository

Publisher copyright

(Article begins on next page)

Partial integration and local mean-field approach for a vector lattice model of microemulsions

C. Buzano,¹ L. R. Evangelista,^{1,2} and A. Pelizzola¹

¹*Dipartimento di Fisica del Politecnico di Torino, Corso Duca degli Abruzzi 24, 10129 Torino, Italy*

²*Departamento de Física, Universidade Estadual de Maringá, Avenida Colombo, 5790, 87020-900, Maringá, Paraná, Brazil*

(Received 6 November 1996)

A vector model on the simple cubic lattice, describing a mixture of water, oil, and amphiphile, is considered. An integration over the amphiphile orientational degrees of freedom is performed exactly in order to obtain an effective Hamiltonian for the system. The resulting model is a three-state (spin-1) system and contains many-site interaction terms. The analysis of the ground state reveals the presence of the water-oil-rich phase as well as the amphiphile-rich and the cubic phases. The temperature phase diagram of the system is analyzed in a local mean-field approach, and a triple line of water-rich, oil-rich, and microemulsion coexistence is obtained. For some values of the model parameters, lamellar phases also appear in the system, but only at finite temperature. The Lifshitz line is determined in a semianalytical way in order to locate the microemulsion region of the disordered phase. [S1063-651X(97)10007-1]

PACS number(s): 82.70.Kj, 05.50.+q, 64.60.Cn

I. INTRODUCTION

Liquid mixtures of water, oil, and amphiphiles (surfactants) have recently been the subject of a very intense investigation [1]. The reason for such an interest is twofold: on the practical side, the characteristic feature of the amphiphiles, that is the presence in the same molecule of a polar head attracting water and a nonpolar tail attracting oil, makes it possible to reduce the water-oil interface tension by several orders of magnitude; on the theoretical side, it is the richness of their phase diagram which makes these mixtures very interesting. At low enough temperatures, in addition to the ordered water-rich and oil-rich phases that are found at low surfactant concentration, for a sufficiently high concentration of surfactant, the liquid mixture can exhibit structured, long-range ordered phases like the lamellar, hexagonal, or cubic phases. At higher temperatures, a reminiscence of these structures is found in the so-called microemulsion. The microemulsion is a region of the disordered phase in which particular short-range correlations are present, and can occur even with low surfactant concentration. In this region oil- and water-occupied microscopic regions are separated by fluctuating layers of amphiphile. The existence of both structured phases and microemulsions is of course due to the basic feature of amphiphiles described above of being molecules with selective ends that tend to be located between oil and water particles.

To distinguish the microemulsion from an ordinary disordered fluid, two criteria have been used in the literature, based on the Lifshitz line [2] or the disorder line [3,4], respectively, which must not be confused. The Lifshitz line is identified by searching the maximum of the water-water scattering amplitude, which is located at nonzero values of the wave number for a microemulsion but not for an ordinary disordered fluid. The disorder line, on the other hand, is given by the condition that the asymptotic decay of the water-water correlation function changes its behavior from monotonic to nonmonotonic. In any case these are not lines of thermodynamic phase transitions. In this paper the border between the microemulsion and the ordinary disordered fluid

will be identified by the Lifshitz line which, in our approach, can be easily calculated.

From the theoretical point of view, the phase diagram and the structure function for the disordered phase have been intensively investigated. Various phenomenological and microscopic models, continuous as well as on the lattice, have been proposed to analyze these systems. Among the lattice models there have been several proposals, put forth by Widom [5], Schick and co-workers [6–8], Matsen and Sullivan [9] (MS in the following) and Ciach, Høye, and Stell [10–15] (CHS from now on). In the model proposed by Widom, three species of molecules occupy the bonds of a lattice; the model can be mapped on an Ising model with extended interactions in which the + and – spins represent water and oil molecules, and the Peierls surfaces separating domains of a given sign represent amphiphilic layers. It is evident that such a model cannot represent neither thick amphiphile layers nor fluctuations in the direction of amphiphilic molecules. In the proposal by Schick and co-workers, a true three-component mixture is introduced, and a three-body interaction term was employed to account for the tendency of the amphiphilic molecules to aggregate water-amphiphile-oil triples. As in the Widom model, however, an orientational degree of freedom for the amphiphile is still missing.

This latter feature was finally introduced by MS and CHS, who dealt with models of three-component mixtures in which amphiphilic molecules carry an additional orientational degree of freedom (which is manifestly not parity invariant), usually constrained to the lattice directions, a great simplification which, however, should not alter the basic thermodynamical properties.

None of the above models is exactly solvable at finite temperature in more than one spatial dimension, and hence they have all been thoroughly investigated by the usual approximate methods of equilibrium statistical mechanics. In particular, the CHS model has been investigated originally by means of the mean-field approximation [10,12], but unfortunately these studies were based on a ground-state analysis [11] which turned out to be incorrect for the simple-cubic lattice case. The correct ground state was determined later

[13] and there soon followed a full, correct mean-field treatment of the case in which a direct amphiphile-amphiphile orientational interaction is absent [14]. Some work was also done on the two-dimensional case [16–19] and, recently, Matsen and Sullivan [19] compared mean-field and Bethe approximations with Monte Carlo simulations on the face-centered-cubic lattice.

An interesting feature of the CHS model is that, in the absence of orientational amphiphile-amphiphile coupling, the corresponding degrees of freedom can be exactly integrated out (summed out, actually). This integration of the simple-cubic lattice CHS model, together with a local mean-field analysis of the resulting Hamiltonian, is the purpose of the present paper. Notice that this program has never been carried out in three dimensions (a short account of a small part of this work has been previously published by us [20]), but only in two dimensions [15], where several important features of these mixtures are missing due to the reduced dimensionality.

This paper is organized as follows. In Sec. II the construction of the Hamiltonian from a multicomponent lattice-gas model is discussed. In Sec. III the exact integration of the orientational degrees of freedom is explicitly performed and the resulting effective spin-1 Hamiltonian is presented. In Sec. IV the general equations for the local mean-field approximation are determined, and the analysis of the uniform phases is presented. In Sec. V we calculate the Lifshitz line, while the phase diagrams are discussed in Sec. VI and, finally, in Sec. VII, we draw our conclusions.

II. MODEL

The CHS model is a vector lattice model in which every site of a cubic lattice is occupied by a particle of some kind (water, oil or amphiphile). The starting point to build up the Hamiltonian of the mixture is to consider the following multicomponent lattice-gas model, in which the orientation-dependent interactions of the amphiphile molecules with oil and water (but not among themselves) have been explicitly included:

$$\mathcal{H} = - \sum_{i,j} \sum_{\mathbf{r},\mathbf{r}'} [\epsilon_{ij}(\mathbf{r}' - \mathbf{r}) N_i(\mathbf{r}) N_j(\mathbf{r}')] - \sum_i \sum_{\mathbf{r}} \mu_i N_i(\mathbf{r}) - \sum_{\mathbf{r}} N_A(\mathbf{r}) \sum_{\mathbf{r}',k} \phi_k[\mathbf{n}(\mathbf{r}) \cdot (\mathbf{r}' - \mathbf{r})] N_k(\mathbf{r}'), \quad (2.1)$$

where $N_j(\mathbf{r}) = 0, 1$ ($j = W, O$, and A) are the occupation-number operators for water (W), oil (O) and amphiphile (A), $\mathbf{n}(\mathbf{r})$ is a unit vector representing the amphiphile orientation which, for the case of a simple-cubic lattice considered here, is restricted to a discrete set of orientations such that it points towards one of the six nearest neighbors of a given site (it is of course meaningless if the site \mathbf{r} is occupied by water or oil), ϵ_{ij} are the coupling energies between the species and ϕ_k ($k = W$ and O) the orientational couplings. The lattice-gas formalism can be transformed into a spin-1 formalism by associating, as customary, the eigenvalues $+1$, -1 , and 0 of the third component of a spin-1 operator $s(\mathbf{r})$ to water, oil, and surfactant, respectively. The

occupation-number operators can then be expressed in terms of the spin-1 operators using Kronecker deltas as

$$\begin{aligned} N_W &= \delta(s(\mathbf{r}), 1) = \frac{1}{2} [s^2(\mathbf{r}) + s(\mathbf{r})], \\ N_O &= \delta(s(\mathbf{r}), -1) = \frac{1}{2} [s^2(\mathbf{r}) - s(\mathbf{r})], \\ N_A &= \delta(s(\mathbf{r}), 0) = 1 - s^2(\mathbf{r}). \end{aligned} \quad (2.2)$$

Now, if we consider only nearest-neighbor interactions and assume (thereby restricting ourselves to balanced systems) that water and oil behave symmetrically (antisymmetrically when interacting with the amphiphile orientational variables, as it must be), that is $\mu_W = \mu_O$, $\epsilon_{WW} = \epsilon_{OO}$, $\epsilon_{OA} = \epsilon_{WA}$, and $\phi_O = -\phi_W$, the Hamiltonian (2.1) can be easily expressed (apart from an irrelevant additive constant) in terms of spin variables as

$$\begin{aligned} \mathcal{H} &= - \frac{J}{2} \sum_{\mathbf{r},\delta} s(\mathbf{r}) s(\mathbf{r} + \delta) - \frac{K}{2} \sum_{\mathbf{r},\delta} s^2(\mathbf{r}) s^2(\mathbf{r} + \delta) + D \sum_{\mathbf{r}} s^2(\mathbf{r}) \\ &\quad - A \sum_{\mathbf{r},\delta} [1 - s^2(\mathbf{r})] s(\mathbf{r} + \delta) \mathbf{n}(\mathbf{r}) \cdot \delta, \end{aligned} \quad (2.3)$$

where δ is a vector of length equal to one lattice spacing pointing toward nearest neighbors. The new parameters are related to the physical coupling energies by the relations

$$\begin{aligned} J &= (\epsilon_{WW} - \epsilon_{WO})/2, \quad K = (\epsilon_{WW} + \epsilon_{WO})/2 + \epsilon_{AA} - 2\epsilon_{WA}, \\ D &= \mu_A - \mu_W + 6(\epsilon_{AA} - \epsilon_{WA}), \quad A = \phi_W. \end{aligned} \quad (2.4)$$

The final Hamiltonian Eq. (2.3) is then characterized by four parameters. The parameter $J > 0$ favors oil-water separation, whereas the sign of the surfactant strength A is not important [more precisely the model is invariant with respect to the transformation $A \rightarrow -A$, $s(\mathbf{r}) \rightarrow -s(\mathbf{r})$], and will be assumed to be positive. We observe that when $A = 0$ the Hamiltonian is of the form of the Blume-Emery-Griffiths [21] (BEG) model.

III. EFFECTIVE MODEL: INTEGRATION OF THE SURFACTANT ORIENTATIONS

As already pointed out, in the model represented by Eq. (2.3) the interaction between amphiphile orientational variables is absent. It is then possible to integrate out exactly the orientational degrees of freedom represented by $\mathbf{n}(\mathbf{r})$ in order to obtain an effective Hamiltonian involving only spin variables and temperature-dependent coupling energies. To accomplish this task, let us rewrite Eq. (2.3) as $\mathcal{H} = \mathcal{H}_{\text{BEG}} + \mathcal{H}_A$, where \mathcal{H}_{BEG} is the Blume-Emery-Griffiths Hamiltonian recovered for $A = 0$, which depends only on the spin-1 variables, while \mathcal{H}_A is the remainder, proportional to A , which accounts for the orientation-dependent interactions.

The partition function can be formally written as

$$\begin{aligned} \mathcal{Z} &= \sum_{\{s(\mathbf{r}), \mathbf{n}(\mathbf{r})\}} e^{-\mathcal{H}} = \sum_{\{s(\mathbf{r})\}} e^{-\mathcal{H}_{\text{BEG}}} \sum_{\{\mathbf{n}(\mathbf{r})\}} e^{-\mathcal{H}_A} \\ &= \sum_{\{s(\mathbf{r})\}} e^{-(\mathcal{H}_{\text{BEG}} + \bar{\mathcal{H}})}, \end{aligned} \quad (3.1)$$

TABLE I. Values of $\zeta(\mathbf{r})$. In the second column we report only one representative permutation, since all permutations are equivalent.

$1-s^2(\mathbf{r})$	$([\Delta_x s(\mathbf{r})]^2, [\Delta_y s(\mathbf{r})]^2, [\Delta_z s(\mathbf{r})]^2)$	$\zeta(\mathbf{r})$	Degeneracy	Symbol
0	\forall	6	1458	
1	(0,0,0)	6	27	ζ_1
1	(0,0,1)	$4+2 \cosh A$	108	ζ_2
1	(0,1,1)	$2+4 \cosh A$	144	ζ_3
1	(1,1,1)	$6 \cosh A$	64	ζ_4
1	(0,0,4)	$4+2 \cosh 2A$	54	ζ_5
1	(0,1,4)	$2+2 \cosh A+2 \cosh 2A$	144	ζ_6
1	(1,1,4)	$4 \cosh A+2 \cosh 2A$	96	ζ_7
1	(1,4,4)	$2 \cosh A+4 \cosh 2A$	48	ζ_8
1	(4,4,4)	$6 \cosh 2A$	8	ζ_9
1	(0,4,4)	$2+4 \cosh 2A$	36	ζ_{10}

where we have absorbed a factor $\beta = (k_B T)^{-1}$ into the model parameters (as a consequence, from now on $1/J$ will represent the reduced temperature), and

$$\overline{\mathcal{H}} = -\ln \sum_{\{\mathbf{n}(\mathbf{r})\}} e^{-\mathcal{H}_A} \quad (3.2)$$

is an effective Hamiltonian which depends only on the spin variables and is calculated in detail below.

As a first step we write, using the fact that the $\{\mathbf{n}(\mathbf{r})\}$ do not interact with each other, $e^{-\overline{\mathcal{H}}} = \prod_{\mathbf{r}} \zeta(\mathbf{r})$, where

$$\begin{aligned} \zeta(\mathbf{r}) &= \sum_{\mathbf{n}(\mathbf{r})} \exp \left\{ A \sum_{\delta} [1-s^2(\mathbf{r})] s(\mathbf{r}+\delta) \mathbf{n}(\mathbf{r}) \cdot \delta \right\} \\ &= 2 \sum_{\alpha=x,y,z} \cosh \{ A [1-s^2(\mathbf{r})] \Delta_{\alpha} s(\mathbf{r}) \} \end{aligned} \quad (3.3)$$

and $\Delta_{\alpha} s(\mathbf{r}) = s(\mathbf{r}+\delta_{\alpha}) - s(\mathbf{r}-\delta_{\alpha})$, with δ_{α} denoting the unit lattice vector along direction α . Considering the $3^7 = 2187$ spin configurations of the cluster formed by a site and its six nearest neighbors, one can see that $\zeta(\mathbf{r})$ can take on only a few different values, which are reported in Table I. Looking at Eq. (3.3) above and at Table I, one realizes that, apart from the coefficient $1-s^2(\mathbf{r})$ which can be easily dealt with, $\zeta(\mathbf{r})$ depends only on $[\Delta_{\alpha} s(\mathbf{r})]^2$, which in turn can take on the values 0, 1, and 4 only, implying that expanding $\zeta(\mathbf{r})$ (and hence also its logarithm) in powers of $[\Delta_{\alpha} s(\mathbf{r})]^2$ one has to retain only terms up to the second order (that is fourth order in the bare differences). On the basis of the above remarks, we introduce the symbols

$$\begin{aligned} P_{klm}(\mathbf{r}) &= [\Delta_x s(\mathbf{r})]^{2k} [\Delta_y s(\mathbf{r})]^{2l} [\Delta_z s(\mathbf{r})]^{2m}, \\ k, l, m &\in \{0, 1, 2\}, \end{aligned} \quad (3.4)$$

and write

$$\overline{\mathcal{H}}(\mathbf{r}) = -\ln \zeta(\mathbf{r})$$

$$= -s^2(\mathbf{r}) \ln 6 - [1-s^2(\mathbf{r})] \sum_{k=0}^2 \sum_{l=0}^2 \sum_{m=0}^2 H_{klm} P_{klm}(\mathbf{r}), \quad (3.5)$$

where the H_{klm} 's are (temperature-dependent, although not manifestly since temperature has been absorbed into the model parameters) coefficients, invariant under permutation of their indices, to be determined. It can be easily checked that there are as many different H_{klm} 's as rows in Table I corresponding to $1-s^2(\mathbf{r})=1$, and thus Eq. (3.5) above can be viewed as a set of ten linear equations in our ten unknown coefficients. Solving the latter with a symbolic manipulator like MATHEMATICA one ends up with

$$H_{klm} = \sum_{r=1}^{10} h_{klm;r} \ln \zeta_r, \quad (3.6)$$

where the $h_{klm;r}$'s are numerical coefficients (again symmetric under permutations of k, l , and m) reported in Table II while the ζ_r have already been given in Table I. The effective Hamiltonian can finally be written as $\overline{\mathcal{H}} = \sum_{\mathbf{r}} \overline{\mathcal{H}}(\mathbf{r})$, and contains multispin interactions (up to seven spins, that is one spin and all its nearest neighbors involved in the same coupling) hidden in the $P_{klm}(\mathbf{r})$ symbols.

IV. THE LOCAL MEAN-FIELD EQUATIONS

The local mean-field equations can be obtained from the approximate total free energy written as a function of the local expectations $m(\mathbf{r}) = \langle s(\mathbf{r}) \rangle$ and $q(\mathbf{r}) = \langle s^2(\mathbf{r}) \rangle$: $F = \sum_{\mathbf{r}} (U(\mathbf{r}) - S(\mathbf{r}))$. We have

$$\begin{aligned} F &= \sum_{\mathbf{r}} \left\{ U(\mathbf{r}) + \left[\mathcal{L} \left(\frac{q(\mathbf{r}) + m(\mathbf{r})}{2} \right) + \mathcal{L}[1 - q(\mathbf{r})] \right. \right. \\ &\quad \left. \left. + \mathcal{L} \left(\frac{q(\mathbf{r}) - m(\mathbf{r})}{2} \right) \right] \right\}, \end{aligned} \quad (4.1)$$

with $\mathcal{L}(x) = x \ln x$. The local energy is

TABLE II. The coefficients $h_{klm;r}$, invariant under permutations of the indices k, l and m .

r klm	1	2	3	4	5	6	7	8	9	10
000	1	0	0	0	0	0	0	0	0	0
001	$-\frac{5}{4}$	$\frac{4}{3}$	0	0	$-\frac{1}{12}$	0	0	0	0	0
002	$\frac{1}{4}$	$-\frac{1}{3}$	0	0	$\frac{1}{12}$	0	0	0	0	0
011	$\frac{25}{16}$	$-\frac{10}{3}$	$\frac{16}{9}$	0	$\frac{5}{24}$	$-\frac{2}{9}$	0	0	0	$\frac{1}{144}$
012	$-\frac{5}{16}$	$\frac{3}{4}$	$-\frac{4}{9}$	0	$-\frac{1}{8}$	$\frac{5}{36}$	0	0	0	$-\frac{1}{144}$
022	$\frac{1}{16}$	$-\frac{1}{6}$	$\frac{1}{9}$	0	$\frac{1}{24}$	$-\frac{1}{18}$	0	0	0	$\frac{1}{144}$
111	$-\frac{125}{64}$	$\frac{25}{4}$	$-\frac{20}{3}$	$\frac{64}{27}$	$-\frac{25}{64}$	$\frac{5}{6}$	$-\frac{4}{9}$	$\frac{1}{36}$	$-\frac{1}{1728}$	$-\frac{5}{192}$
112	$\frac{25}{64}$	$-\frac{65}{48}$	$\frac{14}{9}$	$-\frac{16}{27}$	$\frac{35}{192}$	$-\frac{29}{72}$	$\frac{2}{9}$	$-\frac{1}{48}$	$\frac{1}{1728}$	$\frac{11}{576}$
122	$-\frac{5}{64}$	$\frac{7}{24}$	$-\frac{13}{36}$	$\frac{4}{27}$	$-\frac{11}{192}$	$\frac{5}{36}$	$-\frac{1}{12}$	$\frac{1}{72}$	$-\frac{1}{1728}$	$-\frac{7}{576}$
222	$\frac{1}{64}$	$-\frac{1}{16}$	$\frac{1}{12}$	$-\frac{1}{27}$	$\frac{1}{64}$	$-\frac{1}{24}$	$\frac{1}{36}$	$-\frac{1}{144}$	$\frac{1}{1728}$	$\frac{1}{192}$

$$U(\mathbf{r}) = -\frac{J}{2} \sum_{\delta} m(\mathbf{r})m(\mathbf{r}+\delta) - \frac{K}{2} \sum_{\delta} q(\mathbf{r})q(\mathbf{r}+\delta) + Dq(\mathbf{r}) - [1 - q(\mathbf{r})]g_{\text{AMP}}(\mathbf{r}). \quad (4.2)$$

In Eq. (4.2) the quantity $g_{\text{AMP}}(\mathbf{r})$ can be obtained from Eq. (3.5), as a linear combination of the functions $p_{klm}(\mathbf{r}) = \langle P_{klm}(\mathbf{r}) \rangle$, where the latter expectation has to be evaluated in the local mean-field approximation. Notice that the term in H_{000} cancels with the isolated term $-q(\mathbf{r})\ln 6$ and reduces to an irrelevant constant. For the p_{klm} 's one finds easily that

$$\begin{aligned} p_{001}(\mathbf{r}) &= q(\mathbf{r}+\delta_z) + q(\mathbf{r}-\delta_z) - 2m(\mathbf{r}+\delta_z)m(\mathbf{r}-\delta_z), \\ p_{010}(\mathbf{r}) &= q(\mathbf{r}+\delta_y) + q(\mathbf{r}-\delta_y) - 2m(\mathbf{r}+\delta_y)m(\mathbf{r}-\delta_y), \\ p_{100}(\mathbf{r}) &= q(\mathbf{r}+\delta_x) + q(\mathbf{r}-\delta_x) - 2m(\mathbf{r}+\delta_x)m(\mathbf{r}-\delta_x), \end{aligned} \quad (4.3)$$

$$p_{002}(\mathbf{r}) = q(\mathbf{r}+\delta_z) + q(\mathbf{r}-\delta_z) - 8m(\mathbf{r}+\delta_z)m(\mathbf{r}-\delta_z) + 6q(\mathbf{r}+\delta_z)q(\mathbf{r}-\delta_z),$$

$$p_{020}(\mathbf{r}) = q(\mathbf{r}+\delta_y) + q(\mathbf{r}-\delta_y) - 8m(\mathbf{r}+\delta_y)m(\mathbf{r}-\delta_y) + 6q(\mathbf{r}+\delta_y)q(\mathbf{r}-\delta_y),$$

$$p_{200}(\mathbf{r}) = q(\mathbf{r}+\delta_x) + q(\mathbf{r}-\delta_x) - 8m(\mathbf{r}+\delta_x)m(\mathbf{r}-\delta_x) + 6q(\mathbf{r}+\delta_x)q(\mathbf{r}-\delta_x).$$

The remaining expressions can be calculated from the preceding ones as

$$p_{klm}(\mathbf{r}) = p_{k00}(\mathbf{r})p_{0l0}(\mathbf{r})p_{00m}(\mathbf{r}). \quad (4.4)$$

The free energy can be now minimized with respect to $m(\mathbf{r})$ and $q(\mathbf{r})$ by following standard procedures. This implies to solve the equations resulting from

$$\frac{\partial F}{\partial \xi(\mathbf{r})} = 0, \quad (4.5)$$

where $\xi(\mathbf{r}) = m(\mathbf{r})$ or $q(\mathbf{r})$. From Eq. (4.1), one easily obtains

$$\begin{aligned} \frac{\partial S}{\partial m(\mathbf{r})} &= -\frac{1}{2} \ln \frac{q(\mathbf{r})+m(\mathbf{r})}{q(\mathbf{r})-m(\mathbf{r})}, \\ \frac{\partial S}{\partial q(\mathbf{r})} &= -\frac{1}{2} \ln \frac{[q(\mathbf{r})+m(\mathbf{r})][q(\mathbf{r})-m(\mathbf{r})]}{4[1-q(\mathbf{r})]^2}. \end{aligned} \quad (4.6)$$

After introducing

$$\begin{aligned} a^2(\mathbf{r}) &= \exp \left[-2 \frac{\partial U}{\partial m(\mathbf{r})} \right], \\ b^{-2}(\mathbf{r}) &= \exp \left[-2 \frac{\partial U}{\partial q(\mathbf{r})} \right], \end{aligned} \quad (4.7)$$

and, using Eq. (4.6), Eq. (4.5) can be rewritten as the self-consistent equations

$$\begin{aligned} m(\mathbf{r}) &= \frac{a^2(\mathbf{r}) - 1}{a^2(\mathbf{r}) + a(\mathbf{r})b(\mathbf{r}) + 1}, \\ q(\mathbf{r}) &= \frac{a^2(\mathbf{r}) + 1}{a^2(\mathbf{r}) + a(\mathbf{r})b(\mathbf{r}) + 1}. \end{aligned} \quad (4.8)$$

The evaluation of the partial derivatives of the local energy is presented in the Appendix.

The general approach is remarkably simplified if we restrict for a moment our attention to the uniform phases. It is then possible to determine analytic equations for the critical temperature of the water-oil phase and the corresponding tricritical point, and also to determine the Lifshitz line. To describe the transitions from the water-oil phase to the disordered phase, one can set $m(\mathbf{r}) = m_0$ and $q(\mathbf{r}) = q_0$, and study the free-energy density of uniform phases. If use is made of a magnetic language the disordered phase corresponds to the paramagnetic phase while the water-oil-rich phase is ferromagnetic. Thus, a standard (Landau-Ginzburg) expansion of the free-energy density around the disordered phase characterized by $m_0 = 0$ can be easily performed.

In the uniform case the quantities p_{klm} defined in Eqs. (4.3) and (4.4) become

$$\begin{aligned}
 p_{001} &= p_{010} = p_{100} = 2(q_0 - m_0^2), \\
 p_{002} &= p_{020} = p_{200} = 2q_0 + 6q_0^2 - 8m_0^2, \\
 p_{011} &= p_{101} = p_{110} = p_{001}^2, \\
 p_{012} &= p_{120} = p_{201} = p_{210} = p_{102} = p_{021} = p_{001}p_{002}, \\
 p_{022} &= p_{202} = p_{220} = p_{002}^2, \\
 p_{111} &= p_{001}^3, \\
 p_{112} &= p_{121} = p_{211} = p_{001}^2p_{002}, \\
 p_{122} &= p_{212} = p_{221} = p_{002}^2p_{001}, \\
 p_{222} &= p_{002}^3.
 \end{aligned} \tag{4.9}$$

Therefore the internal energy density can be written down in extended form as

$$\begin{aligned}
 U &= Dq_0 - 3Jm_0^2 - 3Kq_0^2 - (1 - q_0)[3H_{001}p_{001} + 3H_{011}p_{011} \\
 &\quad + 3H_{002}p_{002} + 6H_{012}p_{012} + 3H_{022}p_{022} + H_{111}p_{111}] \\
 &\quad - (1 - q_0)[3H_{112}p_{112} + 3H_{122}p_{122} + H_{222}p_{222}]. \tag{4.10}
 \end{aligned}$$

In an ordinary mean-field treatment like that in Ref. [14], the internal energy density (and hence also the free-energy density) reduces to that of the BEG model. Here this is not so because we have exactly taken into account the fluctuations of the amphiphilic orientational degrees of freedom.

Upon solving the self-consistent equation $\partial F / \partial q_0 = 0$ for q_0 (written as an expansion in powers of m_0) and substituting back into F , one can write the free-energy density in the form of a Ginzburg-Landau expansion as $F = F_0 + F_2m_0^2 + F_4m_0^4 + \dots$. Since q_0 cannot be determined in closed form even for $m_0 = 0$, one has to deal with coefficients F_k which depend on q_0 as well as on the model parameters, with q_0 solution of the equation

$$\begin{aligned}
 D - 6(H_{001} + H_{002}) + a_1q_0 + a_2q_0^2 + a_3q_0^3 + a_4q_0^4 + a_5q_0^5 \\
 + a_6q_0^6 - \ln(1 - q_0) + \ln\left(\frac{q_0}{2}\right) = 0, \tag{4.11}
 \end{aligned}$$

where the coefficients a_i , $i = 1, \dots, 6$ are defined as

$$\begin{aligned}
 a_1 &= 12H_{001} - 24H_{002} - 24H_{011} - 48H_{012} - 24H_{022} - 6K, \\
 a_2 &= 54H_{002} + 36H_{011} - 144H_{012} - 180H_{022} - 24H_{111} - 72H_{112} \\
 &\quad - 72H_{122} - 24H_{222}, \\
 a_3 &= 288H_{012} - 144H_{022} + 32H_{111} - 192H_{112} - 480H_{122} \\
 &\quad - 256H_{222}, \\
 a_4 &= 540H_{022} + 360H_{112} - 360H_{122} - 720H_{222}, \tag{4.12} \\
 a_5 &= 1296H_{122},
 \end{aligned}$$

$$a_6 = 1512H_{222}.$$

As usual in the Ginzburg-Landau formalism, F_2 vanishes at a critical point, while both F_2 and F_4 vanish at a tricritical point, and these equations will be solved numerically in the temperature vs chemical potential plane to obtain the critical curves and tricritical points presented in Sec. VI.

The explicit expression of the coefficient F_2 is

$$\begin{aligned}
 F_2 &= -3J + \frac{1}{2q_0} + 6(1 - q_0)[H_{001} + 4H_{002} \\
 &\quad + 4q_0(H_{011} + 5H_{012} + 4H_{022}) + 4q_0^2(3H_{012} + 12H_{022} \\
 &\quad + H_{111} + 6H_{112} + 9H_{122} + 4H_{222}) \\
 &\quad + 24q_0^3(H_{112} + 5H_{122} + 4H_{222}) \\
 &\quad + 36q_0^4(H_{122} + 4H_{222})], \tag{4.13}
 \end{aligned}$$

while F_4 is too cumbersome to be written in full form, but the equation $F_4 = 0$ can be (apart from a factor of definite sign) written as $\det T = 0$, where T is a 2×2 symmetric matrix of elements

$$\begin{aligned}
 T_{11} &= \frac{1}{3q_0^3} - 48(1 - q_0)[H_{011} + 8H_{012} + 16H_{022} \\
 &\quad + 2q_0(H_{111} + 9H_{112} + 24H_{122} + 16H_{222}) \\
 &\quad + 6q_0^2(H_{112} + 8H_{122} + 16H_{222})], \tag{4.14}
 \end{aligned}$$

$$\begin{aligned}
 T_{12} &= T_{21} = -\frac{1}{2q_0^2} + 6[-H_{001} - 4H_{002} + 4H_{011} + 20H_{012} \\
 &\quad + 16H_{022} + 8q_0(-H_{011} - 2H_{012} + 8H_{022} + H_{111} + 6H_{112} \\
 &\quad + 9H_{122} + 4H_{222}) + 72q_0^2(-3H_{012} - 12H_{022} - H_{111} \\
 &\quad + 21H_{122} + 20H_{222}) + 288q_0^3(-2H_{112} - 7H_{122} + 4H_{222}) \\
 &\quad - 1080q_0^4(H_{122} + 4H_{222})], \tag{4.15}
 \end{aligned}$$

$$\begin{aligned}
 T_{22} &= -3K + \frac{1}{2q_0(1 - q_0)} + 6[H_{001} - 2H_{002} - 2H_{011} - 4H_{012} \\
 &\quad - 2H_{022} + q_0(9H_{002} + 6H_{011} - 24H_{012} - 30H_{022} - 4H_{111} \\
 &\quad - 12H_{112} - 12H_{122} - 4H_{222}) + 4q_0^2(18H_{012} - 9H_{022} \\
 &\quad + 2H_{111} - 12H_{112} - 30H_{122} - 16H_{222}) + 60q_0^3(3H_{022} \\
 &\quad + 2H_{112} - 2H_{122} - 4H_{222}) + 540H_{122}q_0^4 + 756H_{222}q_0^5]. \tag{4.16}
 \end{aligned}$$

V. STRUCTURE FUNCTION AND THE LIFSHITZ LINE

In the disordered fluid phase, the appearance of the short-range correlations which characterize a microemulsion is usually recognized by looking at the structure function; that is, by the momentum space correlation function, or at the real-space correlation function itself. There are two commonly accepted criteria to define a microemulsion. The first one, based on the so-called *disorder line* [3,4], defines as

microemulsion that disordered fluid in which the real space correlation function has the asymptotic behavior

$$g(\mathbf{r}) \equiv \langle s(0)s(\mathbf{r}) \rangle \propto e^{-r/\xi} \cos(kr + \phi), \quad (5.1)$$

with $k \neq 0$ (as usual, ξ denotes the correlation length). This means that, superimposed on the usual exponential decay, we have an oscillatory behavior, which signals that, although long-range order is absent, we still have some short-range structure in which oil- and water-rich regions, separated by a certain amount of amphiphile, can be identified. The locus of points (in the temperature vs concentration, or temperature vs chemical potential plane) at which k vanishes, is called the *disorder line*.

Another criteria for the definition of the microemulsion refers to the so-called *Lifshitz line* [2]. In this case the microemulsion is defined as that disordered fluid in which the water-water structure function $S_{WW}(\mathbf{k})$ (to be defined rigorously below) has a peak at a nonzero wave vector $k_{\text{MAX}} \neq 0$. The locus of points at which $k_{\text{MAX}} = 0$ is then called the *Lifshitz line*. This definition is more related to the experiment than the previous one, $S_{WW}(\mathbf{k})$ being directly measurable by neutron scattering, and we shall adopt it from now on, since in the present approach we have a natural way to determine the Lifshitz line, which is illustrated below.

The water-water structure function is defined as a momentum-space correlation function; in the multicomponent lattice gas, and then in the spin operator formalism we have

$$\begin{aligned} S_{WW}(\mathbf{k}) &= \langle N_W(\mathbf{k})N_W(-\mathbf{k}) \rangle \\ &= \frac{1}{4} \langle [s(\mathbf{k}) + s^2(\mathbf{k})][s(-\mathbf{k}) + s^2(-\mathbf{k})] \rangle. \end{aligned} \quad (5.2)$$

In the mean-field approximation we neglect all correlations, and hence

$$S_{WW}(\mathbf{k}) = \frac{1}{4} (m_{\mathbf{k}}m_{-\mathbf{k}} + q_{\mathbf{k}}q_{-\mathbf{k}} + m_{\mathbf{k}}q_{-\mathbf{k}} + q_{\mathbf{k}}m_{-\mathbf{k}}). \quad (5.3)$$

In order to evaluate explicitly the low moment behavior of the above expression (which in turn is required to locate the Lifshitz line), one usually has to introduce the Fourier expansions of m and q ,

$$\begin{aligned} m(\mathbf{r}) &= m_0 + \delta m(\mathbf{r}) = m_0 + \sum_{\mathbf{k}} m_{\mathbf{k}} e^{i\mathbf{k} \cdot \mathbf{r}}, \\ q(\mathbf{r}) &= q_0 + \delta q(\mathbf{r}) = q_0 + \sum_{\mathbf{k}} q_{\mathbf{k}} e^{i\mathbf{k} \cdot \mathbf{r}}, \end{aligned} \quad (5.4)$$

in the free-energy functional, and to diagonalize the quadratic form which results by an expansion to second order in fluctuations (that is in the Fourier components of m and q). To begin with, we observe that

$$\begin{aligned} \sum_{\mathbf{r}} \delta m(\mathbf{r}) \delta m(\mathbf{r} + \delta \mathbf{r}) &= N \sum_{\mathbf{k}} \cos(\mathbf{k} \cdot \delta \mathbf{r}) m_{\mathbf{k}} m_{-\mathbf{k}}, \\ \sum_{\mathbf{r}} \delta m(\mathbf{r}) \delta q(\mathbf{r} + \delta \mathbf{r}) &= \frac{1}{2} N \sum_{\mathbf{k}} \cos(\mathbf{k} \cdot \delta \mathbf{r}) (q_{\mathbf{k}} m_{-\mathbf{k}} + m_{\mathbf{k}} q_{-\mathbf{k}}). \end{aligned} \quad (5.5)$$

Using the above results we can formally write the leading terms of the expansion in $\{m_{\mathbf{k}}, q_{\mathbf{k}}\}$:

$$\begin{aligned} F &= F_0 + \sum_{\mathbf{k}} [\alpha_{\mathbf{k}} m_{\mathbf{k}} m_{-\mathbf{k}} + \beta_{\mathbf{k}} q_{\mathbf{k}} q_{-\mathbf{k}} \\ &\quad + \gamma_{\mathbf{k}} (m_{\mathbf{k}} q_{-\mathbf{k}} + q_{\mathbf{k}} m_{-\mathbf{k}})] + \dots, \end{aligned} \quad (5.6)$$

where the coefficients $\alpha_{\mathbf{k}}$, $\beta_{\mathbf{k}}$, and $\gamma_{\mathbf{k}}$ have again been calculated with the MATHEMATICA symbolic manipulator. In the disordered phase ($m_0 = 0$) the calculation simplifies considerably, and in particular $\gamma_{\mathbf{k}} = 0$, which means that our quadratic form is already diagonal. The expectations $m_{\mathbf{k}} m_{-\mathbf{k}}$ and $q_{\mathbf{k}} q_{-\mathbf{k}}$ can then be easily obtained by derivation, and one finally has

$$S_{WW}(\mathbf{k}) = \frac{T}{8} (\alpha_{\mathbf{k}}^{-1} + \beta_{\mathbf{k}}^{-1}). \quad (5.7)$$

Expanding (again with MATHEMATICA) the above expression up to second order in \mathbf{k} , one finds $S_{WW}(\mathbf{k}) = S_0 + S_2 k^2 + \dots$, where

$$\begin{aligned} S_2 &= -2Jq_0^2 + 16q_0^2(1 - q_0)[H_{001} + 4H_{002} \\ &\quad + 4q_0(H_{011} + 5H_{012} + 4H_{022}) + 4q_0^2(3H_{012} + 12H_{022} \\ &\quad + H_{111} + 6H_{112} + 9H_{122} + 4H_{222}) \\ &\quad + 24q_0^3(H_{112} + 5H_{122} + 4H_{222}) + 36q_0^4(H_{122} + 4H_{222})]. \end{aligned} \quad (5.8)$$

The Lifshitz line is then the locus of points at which $S_2 = 0$.

VI. PHASE DIAGRAM

The present section will be devoted to a detailed description of the phase diagram that we have obtained in the temperature (that is, $1/J$) vs chemical potential (D/J) and temperature vs surfactant concentration planes, for $K/J = 1$ and several values of A/J .

The free energy, the iterative equations for our variational parameters, and the equations for the Lifshitz line, the critical line, and the tricritical point have already been derived, so the determination of the finite-temperature phase diagram is just a matter of standard numerical work. For fixed values of temperature and chemical potential we have to solve by iteration our local mean-field equations on a suitable cluster, then calculate the free energy of the phases corresponding to the local minima of our functional, and finally compare them in order to find the global minimum and to locate first order phase boundaries and multiphase points. All the results can then be translated into the (experimentally relevant) temperature vs surfactant concentration plane.

On the basis of the ground-state analysis by Ciach, Høye, and Stell [13] we expect pure water-oil, pure surfactant, and cubic (which was named bicontinuous or ordered bicontinuous in previous papers by Ciach and co-workers [13,14] and us [20]) ground states. For $A < (J+K)/2$ there is a boundary between water-oil and surfactant ground states at $D = 3J + 3K$, while for $A > (J+K)/2$ we have the water/oil

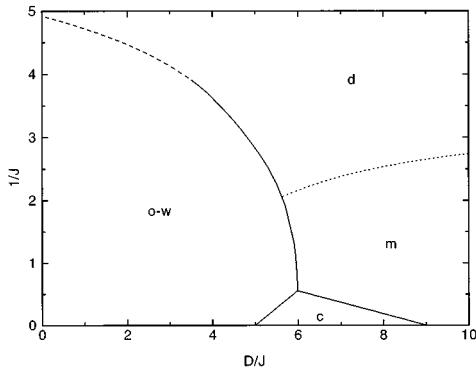


FIG. 1. Phase diagram in the temperature ($1/J$) vs chemical potential (D/J) plane for $K/J=1$ and $A/J=1.5$. Solid, dashed, and dotted lines denote first-order transition, second-order transition and Lifshitz lines respectively. The labels $o-w$, c , m , and d denote oil-water-rich and cubic phases, microemulsion, and usual disordered fluid, respectively.

to cubic boundary at $D=4J+4K-2A$ and the cubic to surfactant boundary at $D=6A$. Furthermore, according to the results by the ordinary (that is, without integration of orientational degrees of freedom) mean-field analysis by Ciach [14] at finite temperature, we eventually expect a few lamellar phases, with different periodicity.

The cubic ground state is obtained by filling three-fourths of the lattice sites by surfactant molecules and the remaining one-fourth by water and oil molecules, which are arranged in a regular, staggered pattern, each species forming a diamond lattice, in such a way that the first and second neighbors of any given water-oil molecule are always surfactants [14]. On the other hand, lamellar states, denoted by L_k in the following, are composed of a regular pattern of k water layers (orthogonal to one lattice direction), a surfactant layer, k oil layers, another surfactant layer, and so on.

Although in principle one could use a huge cubic cluster capable of representing all these phases at the same time, in order to save CPU time it is much more convenient to study the pure phases on a single-site cluster, the cubic phase on a 4^3 cluster with periodic boundary conditions, and the lamellar phases on $L \times 1 \times 1$ clusters of suitable length L [the phase denoted by L_k requires $L=2(k+1)$], again with periodic boundary conditions.

The results of our finite temperature analysis for $K/J=1$ and $A/J=1.5, 3.0$, and 5.0 are reported in Figs. 1–3 in the temperature vs chemical potential plane. The basic structure of the phase diagram is already clear for $A/J=1.5$ (Fig. 1). The cubic phase is separated from the rich phases (both water-oil and surfactant phase) by first-order transition lines, while the water-oil to disordered phase boundary is partly second order and partly first order, exhibiting a tricritical point. All the first-order transition lines meet at a multiphase point, and the Lifshitz line ends in between this point and the tricritical point, that is on the first order part of the water-oil to disordered boundary, giving rise to a line of water-oil-microemulsion coexistence, which is a crucial experimental feature of these systems [1]. Increasing A/J (Figs. 2 and 3) the most evident modification is that the cubic phase (as well as its disordered counterpart, the microemulsion) obviously occupy a larger region of the phase diagram.

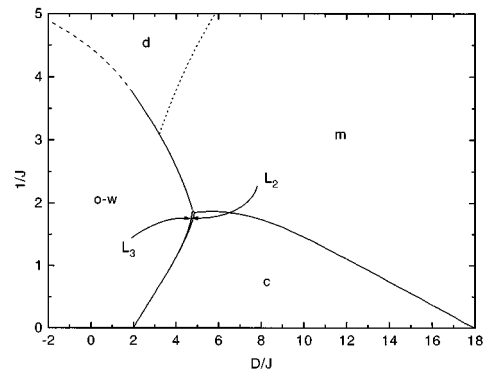


FIG. 2. The same as Fig. 1 for $A/J=3.0$. The labels L_2 and L_3 denote the corresponding lamellar phases.

There is, however, another feature which cannot be expected *a priori*, namely, the appearance of tiny regions occupied by the lamellar phases L_2 and L_3 (we did not consider L_k lamellar phases with $k>3$) close to the multiphase point, on the water-oil side. A similar situation occurs for the case $A/J=2.0$ considered in Ref. [20], with the presence of a small portion of the L_2 phase, which was not found there since we did not look at lamellar phases of higher periodicity than L_1 . We also notice that all the new phase boundaries between the lamellar phases and the adjacent ones are first order. The appearance of such phases can be understood considering that they are stabilized, even in the ground state, by a small interaction between orientational degrees of freedom [13], and hence the small portions of lamellar phase we see here might be continuously connected to the macroscopic region which emerges from the corresponding stable ground state (unfortunately, the present approach cannot enter this region, which would be interesting to study in view of the competition arising between the lamellar and cubic phases).

This situation has to be contrasted with that occurring on the fcc lattice [19], where in the ground state, and hence also in a macroscopic region of the temperature phase diagram, among the structured ordered phases the lamellar phase was found. It has to be noted that these ground-state results are exact, and hence the appearance of different structured ordered phases on different lattices is really a feature of the model, and not of the approximations used.

The phase diagrams in the temperature vs surfactant concentration plane are reported in Figs. 4–6, where all the first-

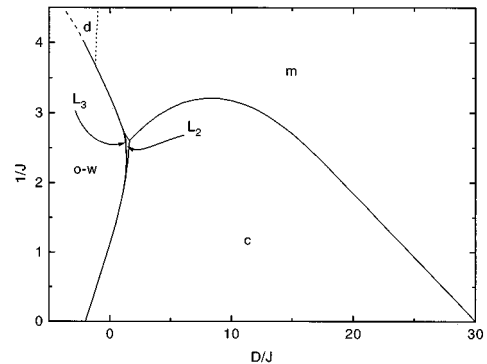


FIG. 3. The same as Fig. 2 for $A/J=5.0$.

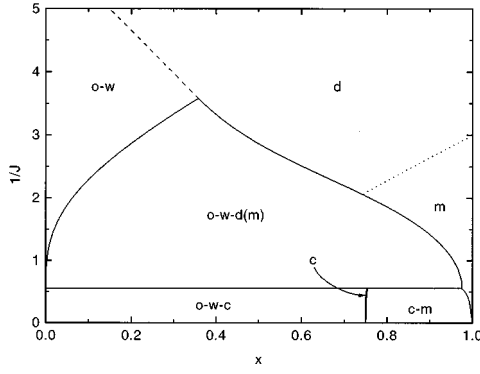


FIG. 4. Phase diagram in the temperature vs surfactant concentration plane for $K/J=1$ and $A/J=1.5$. Solid lines delimit coexistence regions, and dashed and dotted lines denote second-order transition and Lifshitz lines, respectively. The symbol α - β denotes coexistence of phases α and β .

order transition lines have now been replaced by coexistence regions. As it can be expected, increasing the surfactant strength A/J , the region occupied by the microemulsion and the cubic phase enlarges, and for $A/J=5.0$ we find the microemulsion at surfactant concentrations as low as 0.2.

The present results, which can be expected to be more accurate than those previously reported by Ciach [14] because of the exact integration we have performed here, show that, even for $A/J=3.0$ and 5.0 (corresponding to $c/b=1.5$ and 2.5 , respectively in Ciach's paper) there is no critical end point. On the contrary, the rich water-oil to disordered transition exhibits in all cases a tricritical point, and the Lifshitz line ends on the first order part of the transition line instead of ending in the critical end point as found by Ciach. Consequently, even in these cases we have a triple line of oil-water-microemulsion coexistence, which is not found by Ciach, and the cubic to microemulsion transition is always first order in our approach, while Ciach found a tricritical point separating a second order part and a first order part.

VII. CONCLUSIONS

We have studied a vector lattice model proposed by Ciach, Høye, and Stell for microemulsions by means of a partial exact integration and a local mean-field approach, on the simple cubic lattice. The partial integration was possible since the surfactant orientational degrees of freedom were

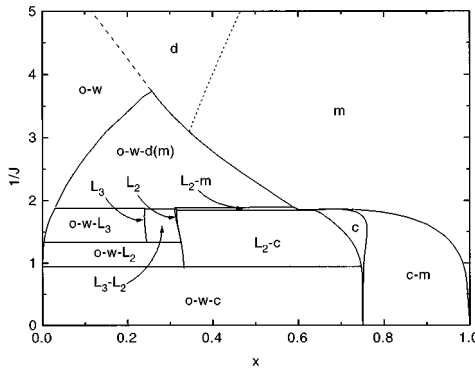


FIG. 5. The same as Fig. 4 for $A/J=3.0$.

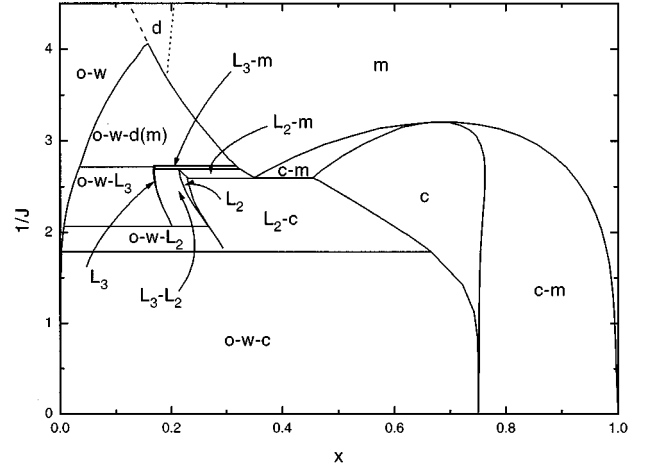


FIG. 6. The same as Fig. 4 for $A/J=5.0$.

assumed not to interact with each other, and was carried out in the three-dimensional case, where it leads to many new multispin (up to seven spins for the simple cubic lattice) interactions, among which one has the three-body interaction introduced by Schick and co-workers on a phenomenological basis [6–8]. The exact integration of the amphiphile orientational degrees of freedom affects the phase diagram even in the region occupied by uniform phases: while in the simple mean-field approximation the orientation-dependent part of the Hamiltonian makes a vanishing contribution to the internal energy of uniform phases, this is no more true if one first performs this exact integration.

In order to characterize the microemulsion region of the disordered phase the Lifshitz line has been calculated, giving a closed-form analytic equation in the model parameters. Similar equations have been derived for the critical and tricritical transitions from the pure water-oil to disordered phase.

The present results can be regarded as an improvement of those previously reported by Ciach [14] in an ordinary mean-field approximation. The main modification is that the critical end-point structure found by Ciach for sufficiently large amphiphilic interaction is replaced here by the more common tricritical point structure, with the Lifshitz line always ending on the first order part of the water-oil to disordered transition line, giving rise to a triple line along which water- and oil-rich phases coexist with the microemulsion.

It would be interesting to apply the present approach to the same model defined on the face-centered-cubic lattice, in order to compare the results with those from simple mean-field approximation and Monte Carlo simulations, and see what kind of improvements are brought in by the exact integration of amphiphile orientations. Finally, since the kind of structured phases that one finds depends strongly on the lattice, it should also be worth looking for structured ordered phases in the ground state of the present model defined on other lattices. Work is in progress along these lines.

APPENDIX

Let us now evaluate the partial derivatives of the local energy, appearing in Eq. (4.7). From Eq. (4.2) one obtains

$$\frac{\partial U}{\partial m(\mathbf{r})} = \{-J[m(\mathbf{r} + \delta_x) + m(\mathbf{r} - \delta_x) + m(\mathbf{r} + \delta_y) + m(\mathbf{r} - \delta_y) + m(\mathbf{r} + \delta_z) + m(\mathbf{r} - \delta_z)] - D_m(\mathbf{r})\},$$

$$\frac{\partial U}{\partial q(\mathbf{r})} = \{D - K[q(\mathbf{r} + \delta_x) + q(\mathbf{r} - \delta_x) + q(\mathbf{r} + \delta_y) + q(\mathbf{r} - \delta_y) + q(\mathbf{r} + \delta_z) + q(\mathbf{r} - \delta_z) + g_{\text{AMP}}(\mathbf{r})] - D_q(\mathbf{r})\}, \quad (\text{A1})$$

where $g_{\text{AMP}}(\mathbf{r})$ was defined in Eq. (4.2) and

$$D_\xi(\mathbf{r}) = \sum_{|\mathbf{r}' - \mathbf{r}|=1} [1 - q(\mathbf{r}')] \frac{\partial g_{\text{AMP}}(\mathbf{r}')}{\partial \xi(\mathbf{r})}, \quad \xi = m, q \quad (\text{A2})$$

(the summation is restricted to nearest neighbors of site \mathbf{r}). Furthermore, from Eqs. (3.5), (4.2), and (4.3), we have

$$\begin{aligned} \frac{\partial g_{\text{AMP}}(\mathbf{r}')}{\partial \xi(\mathbf{r})} &= \sum_{k=1,2} \frac{\partial p_{00k}(\mathbf{r}')}{\partial \xi(\mathbf{r})} R_{00k} + \sum_{k=1,2} \frac{\partial p_{0k0}(\mathbf{r}')}{\partial \xi(\mathbf{r})} R_{0k0} \\ &+ \sum_{k=1,2} \frac{\partial p_{k00}(\mathbf{r}')}{\partial \xi(\mathbf{r})} R_{k00}, \end{aligned} \quad (\text{A3})$$

where

$$\begin{aligned} R_{001} &= H_{001} + H_{011}(p_{010} + p_{100}) + H_{012}(p_{200} + p_{020}) \\ &+ H_{112}(p_{100}p_{020} + p_{200}p_{010}) + H_{122}p_{200}p_{020} \\ &+ H_{111}p_{100}p_{010}, \end{aligned} \quad (\text{A4})$$

$$\begin{aligned} R_{002} &= H_{002} + H_{012}(p_{010} + p_{100}) + H_{022}(p_{020} + p_{200}) \\ &+ H_{112}p_{100}p_{010} + H_{122}(p_{100}p_{020} + p_{200}p_{010}) \\ &+ H_{222}p_{200}p_{020}, \end{aligned}$$

$$\begin{aligned} R_{010} &= H_{001} + H_{011}(p_{001} + p_{100}) + H_{012}(p_{200} + p_{002}) \\ &+ H_{112}(p_{100}p_{002} + p_{200}p_{001}) + H_{122}p_{200}p_{002} \\ &+ H_{111}p_{100}p_{001}, \end{aligned}$$

$$\begin{aligned} R_{020} &= H_{002} + H_{012}(p_{001} + p_{100}) + H_{022}(p_{200} + p_{002}) \\ &+ H_{112}p_{100}p_{001} + H_{122}(p_{100}p_{002} + p_{200}p_{001}) \\ &+ H_{222}p_{200}p_{002}, \end{aligned}$$

$$\begin{aligned} R_{100} &= H_{001} + H_{011}(p_{010} + p_{001}) + H_{012}(p_{020} + p_{002}) \\ &+ H_{112}(p_{010}p_{002} + p_{020}p_{001}) + H_{122}p_{020}p_{002} \\ &+ H_{111}p_{010}p_{001}, \end{aligned}$$

$$\begin{aligned} R_{200} &= H_{002} + H_{012}(p_{010} + p_{001}) + H_{022}(p_{020} + p_{002}) \\ &+ H_{112}p_{010}p_{001} + H_{122}(p_{020}p_{002} + p_{020}p_{001}) \\ &+ H_{222}p_{020}p_{002}. \end{aligned}$$

It remains to calculate, directly from Eq. (4.3), the derivatives

$$\frac{\partial p_{00k}(\mathbf{r}')}{\partial m(\mathbf{r})} = -2k^2[\delta_{\mathbf{r}, \mathbf{r}'} + \delta_z m(\mathbf{r}' - \delta_z) + \delta_{\mathbf{r}, \mathbf{r}' - \delta_z} m(\mathbf{r}' + \delta_z)],$$

$$\frac{\partial p_{0k0}(\mathbf{r}')}{\partial m(\mathbf{r})} = -2k^2[\delta_{\mathbf{r}, \mathbf{r}'} + \delta_y m(\mathbf{r}' - \delta_y) + \delta_{\mathbf{r}, \mathbf{r}' - \delta_y} m(\mathbf{r}' + \delta_y)], \quad (\text{A5})$$

$$\frac{\partial p_{k00}(\mathbf{r}')}{\partial m(\mathbf{r})} = -2k^2[\delta_{\mathbf{r}, \mathbf{r}'} + \delta_x m(\mathbf{r}' - \delta_x) + \delta_{\mathbf{r}, \mathbf{r}' - \delta_x} m(\mathbf{r}' + \delta_x)]$$

and

$$\begin{aligned} \frac{\partial p_{00k}(\mathbf{r}')}{\partial q(\mathbf{r})} &= \delta_{\mathbf{r}, \mathbf{r}'} + \delta_z [1 + 6\delta_{k,2}q(\mathbf{r}' - \delta_z)] \\ &+ \delta_{\mathbf{r}, \mathbf{r}' - \delta_z} [1 + 6\delta_{k,2}q(\mathbf{r}' + \delta_z)], \end{aligned}$$

$$\begin{aligned} \frac{\partial p_{0k0}(\mathbf{r}')}{\partial q(\mathbf{r})} &= \delta_{\mathbf{r}, \mathbf{r}'} + \delta_y [1 + 6\delta_{k,2}q(\mathbf{r}' - \delta_y)] \\ &+ \delta_{\mathbf{r}, \mathbf{r}' - \delta_y} [1 + 6\delta_{k,2}q(\mathbf{r}' + \delta_y)], \end{aligned} \quad (\text{A6})$$

$$\begin{aligned} \frac{\partial p_{k00}(\mathbf{r}')}{\partial q(\mathbf{r})} &= \delta_{\mathbf{r}, \mathbf{r}'} + \delta_x [1 + 6\delta_{k,2}q(\mathbf{r}' - \delta_x)] \\ &+ \delta_{\mathbf{r}, \mathbf{r}' - \delta_x} [1 + 6\delta_{k,2}q(\mathbf{r}' + \delta_x)]. \end{aligned}$$

[1] G. Gompper and M. Schick, in *Phase Transitions and Critical Phenomena*, edited by C. Domb and J. L. Lebowitz (Academic, London, 1994), Vol. 16.
[2] R. M. Hornreich, M. Luban, and S. Shtrikman, *Phys. Rev. Lett.* **35**, 1678 (1975).
[3] M. E. Fisher and B. Widom, *J. Chem. Phys.* **50**, 3756 (1969).
[4] J. Stephenson, *J. Math. Phys. (N.Y.)* **11**, 420 (1970).
[5] B. Widom, *J. Chem. Phys.* **84**, 6943 (1986).
[6] M. Schick and W.-H. Shih, *Phys. Rev. Lett.* **59**, 1205 (1987).
[7] G. Gompper and M. Schick, *Phys. Rev. Lett.* **62**, 1647 (1989); *Phys. Rev. B* **41**, 9148 (1990).

[8] M. Schick, *Physica A* **172**, 200 (1991).
[9] M. W. Matsen and D. E. Sullivan, *Phys. Rev. A* **41**, 2021 (1990); **44**, 3710 (1991).
[10] A. Ciach, J. S. Høye, and G. Stell, *J. Phys. A* **21**, L777 (1988).
[11] A. Ciach, J. S. Høye, and G. Stell, *J. Chem. Phys.* **90**, 1214 (1989).
[12] A. Ciach, J. S. Høye, and G. Stell, *J. Chem. Phys.* **90**, 1222 (1989).
[13] A. Ciach and J. S. Høye, *J. Chem. Phys.* **95**, 5300 (1991).
[14] A. Ciach, *J. Chem. Phys.* **96**, 1399 (1992).
[15] M. S. Skaf and G. Stell, *J. Chem. Phys.* **97**, 7699 (1992).

- [16] M. Laradji, H. Guo, M. Grant, and M. Zuckermann, Phys. Rev. A **44**, 8184 (1991).
- [17] P. A. Slotte, Phys. Rev. A **46**, 6469 (1992).
- [18] M. W. Matsen, Phys. Rev. E **48**, 2292 (1993).
- [19] M. W. Matsen and D. E. Sullivan, Phys. Rev. E **51**, 548 (1995).
- [20] C. Buzano, L. R. Evangelista, and A. Pelizzola, Mol. Cryst. Liq. Cryst. **290**, 41 (1996).
- [21] M. Blume, V. Emery, and R. B. Griffiths, Phys. Rev. A **4**, 1071 (1971).